



# Bis(Alumanyl)Magnesium: a Source of Nucleophilic or Radical Aluminium-Centred Reactivity

Liam P. Griffin, Mathias A. Ellwanger, Jonathon Clark, William K. Myers, Aisling F. Roper, Andreas Heilmann, and Simon Aldridge\*

**Abstract:** The homoleptic magnesium bis(alumanyl) compound  $\text{Mg}[\text{Al}(\text{NON})]_2$  ( $\text{NON} = 4,5\text{-bis}(2,6\text{-diisopropylanilido})\text{-}2,7\text{-di-tert-butyl-}9,9\text{-dimethylxanthene}$ ) can be accessed from  $\text{K}_2[\text{Al}(\text{NON})]_2$  and  $\text{MgI}_2$  and shown to possess a non-linear geometry ( $\angle\text{Al-Mg-Al} = 164.8(1)^\circ$ ) primarily due to the influence of dispersion interactions. This compound acts as a four-electron reservoir in the reductive de-fluorination of  $\text{SF}_6$ , and reacts thermally with polar substrates such as  $\text{MeI}$  via nucleophilic attack through aluminium, consistent with the QT-AIM charges calculated for the metal centres, and a formal description as a  $\text{Al(I)-Mg(II)-Al(I)}$  trimetallic. On the other hand, under photolytic activation, the reaction with 1,5-cyclooctadiene leads to the stereo-selective generation of transannular cycloaddition products consistent with radical based chemistry, emphasizing the covalent nature of the  $\text{Mg-Al}$  bonds and a description as a  $\text{Al(II)-Mg(0)-Al(II)}$  synthon. Consistently, photolysis of  $\text{Mg}[\text{Al}(\text{NON})]_2$  in hexane in the absence of COD generates  $[\text{Al}(\text{NON})]_2$  together with magnesium metal.

Within this field, a number of systems have recently been reported which take the assembly of covalent metal-metal bonds of this sort one step further by defining trimetallic ‘chains’ in which a (two-coordinate) central metal atom can be viewed as possessing a formal oxidation state of zero (Figure 1). These include both homo- and hetero-trimetallic compounds (**I–III**),<sup>[7,8]</sup> each of which has been described in terms of a  $\text{M(I)-M'(0)-M(I)}$  formalism. Beyond the divalent metals of groups 2 and 12, related  $s/p$  block examples are rare;  $\text{MAl}_2$  and  $\text{MGa}_2$  systems **IV** and **V** have been synthesized by Fischer by insertion of neutral  $\text{Al(I)}$  or  $\text{Ga(I)}$  moieties into  $\text{M-X}$  bonds ( $\text{M} = \text{Zn, Hg}$ ;  $\text{X} = \text{CH}_3, \text{SC}_6\text{F}_5, \text{N}(\text{SiMe}_3)_2$ ),<sup>[9–11]</sup> and systems featuring additional Lewis bases coordinated at the central metal also have literature precedent.<sup>[12]</sup>

Within this sphere, we perceived that the recent synthesis of nucleophilic  $\text{Al(I)}$  (‘alumanyl’) anions might offer an alternative route to access  $\text{M-Al}$  bonds featuring a wide range of metals.<sup>[13,14]</sup> While this has proved to be synthetically viable, the only trimetallic bis(alumanyl) systems reported to date via this approach (to our knowledge) are the potassium bis(alumanyl)-cuprate **VI**, synthesized from

**M**etal-metal bonded systems have played a central role in the recent development of main group chemistry,<sup>[1]</sup> both from a fundamental perspective in providing the driver for new models of electronic structure/bonding,<sup>[2]</sup> and from the viewpoint of defining new patterns of reactivity towards small molecules.<sup>[3]</sup> Landmark examples include Power’s digermene,  $\text{Ar}^{\text{Dipp}}\text{GeGeAr}^{\text{Dipp}}$  ( $\text{Ar}^{\text{Dipp}} = 2,6\text{-Dipp}_2\text{C}_6\text{H}_3$ ;  $\text{Dipp} = 2,6\text{-}^i\text{Pr}_2\text{C}_6\text{H}_3$ ) and related tin compounds which enabled unprecedented main group activation of  $\text{H}_2$ ,<sup>[4]</sup> together with Carmona’s  $(\eta^5\text{-C}_5\text{Me}_5)\text{ZnZn}(\eta^5\text{-C}_5\text{Me}_5)$  and Jones’  $(\text{Nacnac}^{\text{Dipp}})\text{MgMg}(\text{Nacnac}^{\text{Dipp}})$  ( $\text{Nacnac}^{\text{Dipp}} = \text{HC}(\text{MeCDippN})_2$ ) which accessed previously ill-defined oxidation states for these pre- and post-transition elements.<sup>[5,6]</sup>

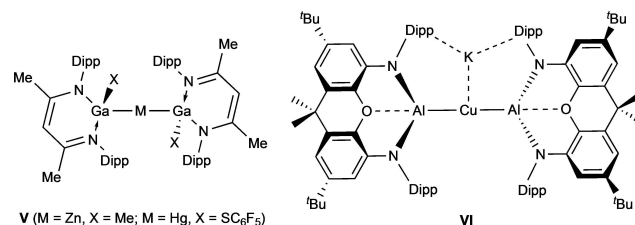
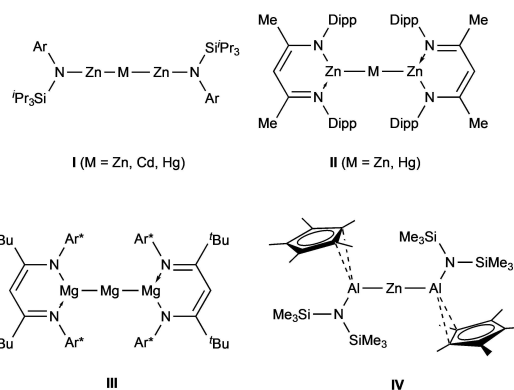


**Figure 1.** Selected covalently bonded trimetallic compounds of relevance to the current study. ( $\text{Ar} = \text{C}_6\text{H}_2\text{-Me-4-(CHPh)}_2\text{-}2,6$ ;  $\text{Ar}^* = \text{C}_6\text{H}_3\text{-(CHEt)}_2\text{-}2,6$ ).

[\*] L. P. Griffin, Dr. M. A. Ellwanger, J. Clark, Dr. W. K. Myers, A. F. Roper, Dr. A. Heilmann, Prof. S. Aldridge  
Inorganic Chemistry Laboratory, Department of Chemistry  
University of Oxford  
South Parks Road, Oxford, OX1 3QR (UK)  
E-mail: simon.aldrige@chem.ox.ac.uk

© 2024 The Authors. Angewandte Chemie published by Wiley-VCH GmbH. This is an open access article under the terms of the Creative Commons Attribution License, which permits use, distribution and reproduction in any medium, provided the original work is properly cited.

$K_2[Al(NON)]_2$  and  $Ph_3PCuI$ , and a very recently reported bis(alumanyl) samarium complex reported by Yamashita and co-workers.<sup>[11,14d]</sup> With a view to extending this approach, to allow for systematic exploration of the electronic structure and reactivity of Al–M–Al containing systems, we report here on the synthesis of the bis(alumanyl) magnesium complex  $Mg[Al(NON)]_2$ . This compound provides an interesting counterpoint to existing alumanyl chemistry by offering experimental evidence for radical chemistry in addition to nucleophilic behaviour at aluminium.

Reaction of a toluene solution of potassium alumanyl compound **1**<sup>[13a]</sup> with a slurry containing ca. 0.6 equiv. (by metal) of  $MgI_2$  over a period of 14 h leads to the formation of a new pale yellow species, characterized by two Dipp  $CH_3$  and one CH signal in its  $^1H$  NMR spectrum in  $C_6D_6$ . Recrystallization from pentane gives a yellow crystalline product in ca. 80 % yield (0.15 g scale), which has been characterized by multinuclear NMR, IR and elemental microanalysis. X-ray diffraction studies on single crystals obtained from pentane or benzene solution reveal it to be the magnesium bis(alumanyl) complex  $Mg[Al(NON)]_2$  (**2**; Scheme 1 and Figure 2). As such, **2** represents a very rare example of complex featuring a wholly alumanyl supporting ligand set.<sup>[10,14d]</sup>

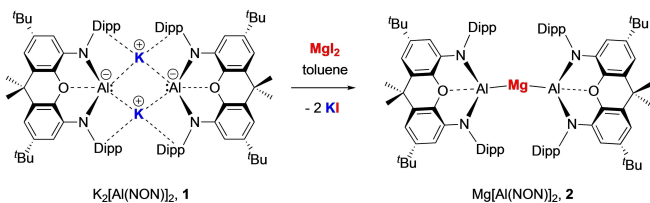
From a geometric perspective, the molecular structure of **2** is defined by a bent coordination geometry at magnesium ( $\angle Al-Mg-Al = 164.8(1)^\circ$ ; Figure 2). The corresponding angles at the central metal atom in the other two known homoleptic bis(alumanyl) complexes are closer to linear: bis(alumanyl)zinc system **IV** has a *crystallographically imposed* linear geometry at zinc, while the bis-

(alumanyl)cuprate  $K[Cu\{Al(NON)_2\}]$  (**VI**), features an angle of  $174.9(1)^\circ$  at copper, albeit with the positioning of the  $K^+$  counterion between the flanking Dipp groups presumably contributing to the alignment of the ligand scaffold.<sup>[14d]</sup>

In the case of **2**, the bending at magnesium away from linearity, while reminiscent of the bent structures observed for the heavier alkaline earth dihalides in the gas phase,<sup>[15]</sup> is thought primarily result from dispersion interactions involving the flanking Dipp groups of the NON supporting ligands. As such (i) close contacts are observed between  $^iPr$  groups associated with the two different  $Al(NON)$  metallo-ligands in the ‘pocket’ formed by bending the Al–Mg–Al unit (closest H...H contacts: 2.35, 2.37 Å; closest C...C contacts: 3.792(3), 3.857(3) Å); (ii) the molecular structure of **2** is modelled well by quantum chemical calculations employing Grimme’s empirical dispersion correction (along with PBE1PBE hybrid exchange functional and Def2-SVP basis set):<sup>[16]</sup>  $\angle Al-Mg-Al = 158.9^\circ$ ;  $d(Al-Mg) = 2.682, 2.694$  Å (cf. 2.695(1) and 2.689(1) Å); and (iii) the corresponding minimum energy structure optimized without accounting for dispersion (but using an otherwise identical method) involves a significantly wider Al–Mg–Al angle ( $172.0^\circ$ ).

The Mg–Al bond lengths determined for **2** (2.695(1) and 2.689(1) Å) are comparable to the sum of the respective covalent radii ( $1.41 + 1.21$  Å),<sup>[17]</sup> but very short compared to those reported for other Mg–Al systems (six examples in the range 2.727(2)–2.7980(6) Å).<sup>[18]</sup> The only system featuring a comparable metal-metal separation is  $(Nacnac^{Mes})Mg-Al(NON)$  (2.696(1) Å;  $Nacnac^{Mes} = HC(MeCMesN)_2$ ),<sup>[13a]</sup> which features the same alumanyl ‘metallo-ligand’. Compared to this system, **2** might be expected to feature a shorter Mg–Al bond on account of the reduced coordination number at magnesium (i.e. two vs. three); on the other hand the mutually *trans* disposition of the two alumanyl units in **2**, and the strong  $\sigma$  donor capabilities of the  $Al(NON)$  fragment,<sup>[14d]</sup> might be expected to influence the Mg–Al separation in the opposite sense.

Quantum chemical calculations also show that the HOMO and LUMO for **2** are best described, respectively, as a Mg–Al  $\sigma$  bonding orbital and an (unoccupied) in-phase  $\pi$  orbital which is delocalized over all three metal atoms (Figures 3 and s10). The associated HOMO energy ( $-6.44$  eV) is significantly lower than determined, for example, for  $(Et_2O)_2Li-Al(NON)$  ( $-4.12$  eV), reflecting a higher degree of covalency in the Al–M bonds. Consistently,



**Scheme 1.** Synthesis of bis(alumanyl) magnesium complex **2** from potassium alumanyl dimer **1** via metathesis.

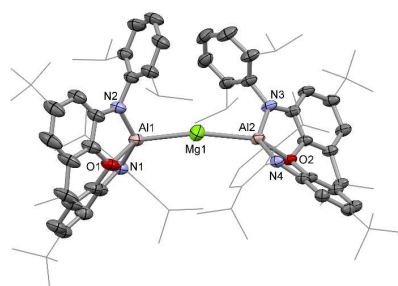


**Figure 2.** Molecular structure of **2** in the solid state as determined by X-ray crystallography. Thermal ellipsoids set at 50% probability; H atoms and solvent molecules omitted, and selected substituents shown in wireframe format for clarity. Key bond lengths (Å) and angles ( $^\circ$ ): Mg–Al 2.695(1), 2.689(1); Al–N 1.900(1), 1.901(1), 1.902(1), 1.904(1); Al–O 2.001(1), 2.014(1); Al–Mg–Al 164.8(1).

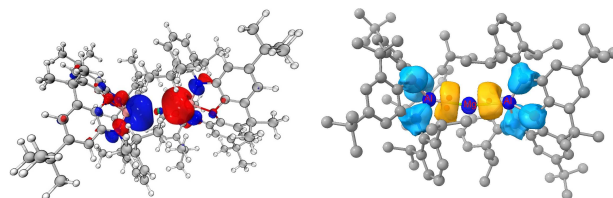


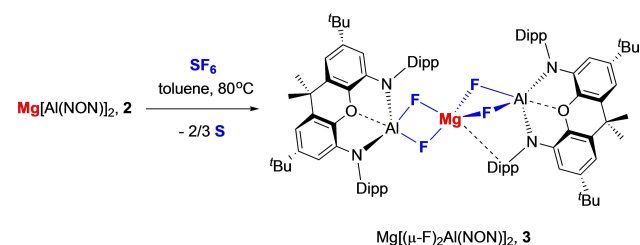
**Figure 3.** (left) DFT calculated HOMO ( $-6.44$  eV) for **2**. (Iso-value = 0.03; PBE1PBE hybrid exchange functional, Def2-SVP basis set, Grimme empirical dispersion correction). (right) ELF iso-surface for compound **2** (0.6 a.u.). Key: Yellow = metal-metal bond basins, Blue = ligand based basins.

QT-AIM calculations reveal bond critical points between Mg and each Al centre, with associated electron densities ( $\rho(r) = 0.037, 0.038 \text{ e } \text{\AA}^{-3}$ ) that are similar to that determined for (Nacnac<sup>Mes</sup>)Mg–Al(NON) ( $0.036 \text{ e } \text{\AA}^{-3}$ ), and intermediate between those calculated for (Et<sub>2</sub>O)<sub>2</sub>Li–Al(NON) ( $0.019 \text{ e } \text{\AA}^{-3}$ ) and (Nacnac<sup>Mes</sup>)Zn–Al(NON) ( $0.060 \text{ e } \text{\AA}^{-3}$ ).<sup>[19]</sup> The NAO orbital occupancy determined for the Mg 3s orbital is 0.815 e (together with 0.023 e for Mg 3p), which can be compared to 0.46 e for the Mg 3s orbital in (Nacnac<sup>Mes</sup>)Mg–Al(NON), which features a single aluminyl ‘metallo-ligand.’ ELF calculations reveal the presence of two metal-metal bonding basins for **2** (Figure 3) containing 1.948 and 1.965 electrons.

Trimagnesium compound **III** (Figure 1) has been described in terms of a Mg(I)–Mg(0)–Mg(I) formalism, reflecting the essentially non-polar nature of Mg–Mg bonds, and QT-AIM calculated charges of +0.90/+0.36/+0.90 (when allowance is made for the presence of two non-nuclear attractors).<sup>[8]</sup> By means of comparison, **2** features a significantly higher charge at the central Mg atom (+1.36 vs. +0.36; Al charges: +1.08/+1.10), and, as a consequence, Mg–Al bonds which are polarized in the sense Mg( $\delta^+$ )–Al( $\delta^-$ ), consistent with the respective Pauling electronegativities (Al: +1.61; Mg: +1.31). Insofar as formal oxidation states can be assigned with any reliability, a formalism as Al(I)–Mg(II)–Al(I) would therefore seem most appropriate in the case of **2**. Further attempts to probe the electronic structure of **2** experimentally were carried out by examining its patterns of reactivity with respect to polar, oxidizing or unsaturated substrates.

**2** is found to be intrinsically less reactive than **1** towards non-polar (or weakly polar) substrates, showing no propensity to activate H<sub>2</sub> or arenes such as benzene under thermal conditions. The more covalent nature of the metal aluminium interaction and accompanying stabilization of the HOMO are presumably of key importance. The capabilities of **2** as a four-electron reductant are, however, signaled by its reactivity towards the kinetically inert substrate SF<sub>6</sub>, with which it reacts at 80 °C over a period of 48 h to give Mg[( $\mu$ -F)<sub>2</sub>Al(NON)]<sub>2</sub> (**3**; Scheme 2).

At room temperature **3** gives rise to broad resonances in the <sup>1</sup>H NMR spectrum, and to two broad signals in the <sup>19</sup>F NMR spectrum at ca. –170 ppm, i.e. in the expected range for aluminium-bound fluorides. X-ray diffraction studies on single crystals obtained from benzene confirm the presence



**Scheme 2.** Reaction of bis(aluminyl)magnesium complex **2** with SF<sub>6</sub> to generate mixed aluminium/magnesium fluoride complex Mg[( $\mu$ -F)<sub>2</sub>Al(NON)]<sub>2</sub>, **3**.

of Al–F bonds (Figure 4), and show that **3** is derived from the formal addition of F<sub>2</sub> across both of the Al–Mg bonds in **2**, via the reductive defluorination of SF<sub>6</sub>. No (NON)Al/S containing species could be detected spectroscopically in solution, and the fate of the sulphur component under these conditions is thought to be as amorphous sulphur precipitate observed in the reaction mixture. Consistently, carrying out the reaction in the presence of PPh<sub>3</sub> leads to the formation of PPh<sub>3</sub>S.

The structure of **3** is unusual in containing an MgF<sub>2</sub> fragment, formally encapsulated between two [(NON)AlF] units. Despite the high lattice enthalpy of MgF<sub>2</sub> (ca. 2960 kJ mol<sup>-1</sup>),<sup>[20]</sup> the presence of strong Al–F interactions presumably serves to prevent further aggregation. The coordination environment at the aluminium centres lies between trigonal bipyramidal and square pyramidal ( $\tau = 0.66, 0.59$  for Al1/Al2) with the Al–F distances associated with the axial sites (F1, F3) being somewhat longer than those involving the equatorial fluorides (1.796(1)/1.821(1) vs. 1.769(1)/1.773(1) Å). The coordination environment at magnesium is significantly distorted from tetrahedral; the Mg–F bond lengths are grouped into two sets (1.894(1)/1.902(1) and 1.920(2)/1.919(2) Å), with the shorter bonds being associated with the fluoride ligands which are more weakly bound at aluminium (i.e. F1 and F3, the axial fluorides). Moreover, the Dipp group of one NON ligand interacts weakly with Mg1 ( $d(\text{Mg}\cdots\text{C}_{24}) = 3.197(3) \text{ \AA}$ ) - in an orientation roughly *trans* to F4. The remaining three fluorides (F1–F3) and Mg1 lie in an approximately planar arrangement, with the mean deviation from the least squares plane being 0.059 Å. As such, the coordination geometry at

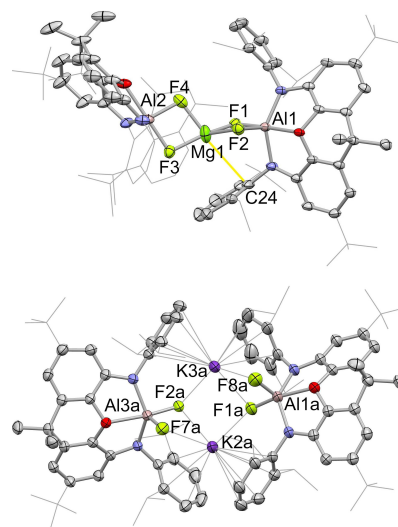


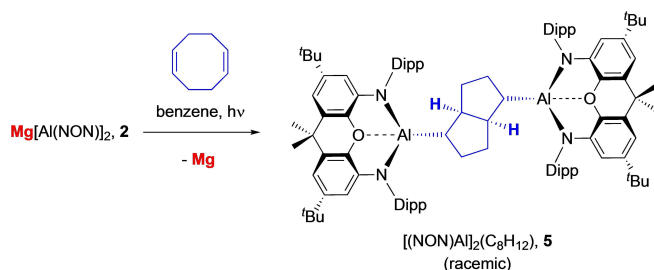
**Figure 4.** Molecular structures of Mg[( $\mu$ -F)<sub>2</sub>Al(NON)]<sub>2</sub> (**3**, upper) and K<sub>2</sub>[(NON)AlF<sub>2</sub>] (**4**, lower) in the solid state as determined by X-ray crystallography. Thermal ellipsoids set at 50% probability; H atoms and solvent molecules omitted, and selected substituents shown in wireframe format for clarity. Key bond lengths (Å): (for **3**) Al–F 1.796(1), 1.821(1), 1.769(1), 1.773(1); Mg–F 1.894(1), 1.902(1), 1.920(2), 1.919(2); Mg $\cdots$ C<sub>24</sub> 3.197(3); (for **4**) Al–F 1.753(1), 1.709(1), 1.756(1), 1.755(1), K $\cdots$ F 2.875(1), 2.723(1), 2.625(1), 2.652(1), 2.681(1), 3.160(1).

Mg1 could be viewed as tending towards trigonal bipyramidal, with F4 and the C24 formally constituting the axial ligands. In solution, the fluoride ligands undergo fluxional exchange, being rendered equivalent on the NMR timescale at 343 K, and being resolved into an AB multiplet below 273 K (ESI, Figure S8).

This mode of reactivity of **2** is also common to potassium aluminyl compound **1**, which reductively defluorinates SF<sub>6</sub> in similar fashion generating the potassium difluoroaluminate dimer K<sub>2</sub>[(NON)AlF<sub>2</sub>] (**4**), albeit under somewhat milder conditions (room temperature, 5 min). **4** is isostructural with the corresponding dihydride K<sub>2</sub>[(NON)AlH<sub>2</sub>], with the K<sup>+</sup> cations held in place by a combination of K...F (2.625(1)–3.160(1) Å) and K...arene interactions (3.177(2)–3.392(2) Å; Figure 4). Crimin and co-workers have previously reported SF<sub>6</sub> activation by {HC(MeCDippN)<sub>2</sub>}Al.<sup>[20]</sup>

The reduction chemistry observed with **2** reflects the availability of a four-electron reservoir constituted by the two Mg–Al bonds. Furthermore, the polarity of these bonds (and a formalism for **2** as Al(I)–Mg(II)–Al(I)) implied by the QT-AIM charge distribution is supported by reactions with electrophiles such as methyl iodide. The reaction of **2** with MeI in benzene-d<sub>6</sub> solution selectively generates (NON)AlMe, in a manner analogous to the reaction of potassium system **1** with methyl iodide,<sup>[13a]</sup> and implies that the aluminium centres in each case behave in a nucleophilic manner.

By contrast, the reactivity of **2** towards 1,5-cyclooctadiene (COD) implies that other factors can also be important in driving product formation *under photolytic conditions*. While **1** reacts with alkenes rapidly at room temperature via [2+1] cycloaddition chemistry to generate the corresponding metallacyclo-propanes,<sup>[13c]</sup> **2** does not react with COD even under more forcing thermal conditions (72 h at 80 °C). On the other hand, broadband UV photolysis of a solution in C<sub>6</sub>D<sub>6</sub> (Hg arc lamp, 191–360 nm, 125 W) leads to generation of a single major NON-containing species, as judged by *in situ* <sup>1</sup>H NMR monitoring, together with magnesium metal (Scheme 3). Single crystals of the (extremely sensitive) aluminium-containing product suitable for X-ray crystallography were grown from a concentrated benzene solution, and shown to contain a racemic mixture of (*R,R,R,R*) and (*S,S,S,S*) 2,6-dimetallated *cis*-bicyclo[3.3.0]octanes (Figure 5). Structurally, the product



**Scheme 3.** Reaction of bis(aluminyl) magnesium complex **2** with 1,5-cyclooctadiene under UV photolysis to generate the racemic (*R,R,R,R*) and (*S,S,S,S*) 2,6-dimetallated *cis*-bicyclo[3.3.0]octane, [(NON)Al]<sub>2</sub>(C<sub>8</sub>H<sub>12</sub>) (**5**).

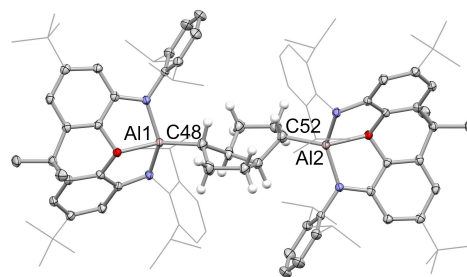


**Figure 5.** Molecular structure of [(NON)Al]<sub>2</sub>(C<sub>8</sub>H<sub>12</sub>) (**5**) in the solid state as determined by X-ray crystallography. Thermal ellipsoids set at 50% probability; most H atoms omitted and selected substituents shown in wireframe format for clarity. Key bond lengths (Å): Al–C 1.948(5), 1.952(5); C–C (within bicyclooctane unit) 1.51(1), 1.531(8), 1.532(9), 1.550(4), 1.518(8), 1.531(8), 1.52(1), 1.542(7).

**5** features a *cis*-bicyclo[3.3.0]octane core with chemically equivalent [Al(NON)] fragments bound in the 2- and 6-positions, each adopting pseudo-equatorial positions with respect to the C<sub>8</sub> skeleton, in line with steric considerations. The Al–C and C–C bonds within the organometallic core conform to the expected distances for the respective single bonds.<sup>[17]</sup>

Mechanistically, the formation of **5** from **2** and 1,5-cyclooctadiene constitutes a transannular 1,5-cycloaddition reaction involving the creation of four contiguous stereocentres in one step; the crystalline product features a racemic mixture of (*R,R,R,R*) and (*S,S,S,S*) forms.<sup>[22]</sup> This mode of reactivity (and selectivity) is strongly characteristic of free radical transannular cyclization processes of 1,5-cyclooctadiene, being widely preceded for classical organic radical systems derived from peroxides, chlorocarbons or carbonyl compounds.<sup>[23]</sup> Thus, for example, the reaction of COD with CCl<sub>4</sub> under UV photolysis generates the analogous cycloaddition product 2-trichloromethyl-6-chloro-*cis*-bicyclo-[3.3.0]octane. Indeed, related studies have invoked the formation of bicyclic systems of this type from cyclooctene precursors as a mechanistic probe for radical-based chemistry.<sup>[24]</sup> The stereo-selective formation of **5** from **2** is therefore consistent with the transient formation of Al(II) radical species under photolytic conditions, and with the concurrent generation of magnesium metal.<sup>[25]</sup>

Consistent with this assertion: (i) photolysis of **2** in the absence of COD in hexane solution generates the (known) Al(II) dimer (NON)Al–Al(NON),<sup>[13a]</sup> together with metallic magnesium; (ii) radical species featuring well-defined <sup>27</sup>Al hyperfine couplings are generated from **2** when it is photolyzed in benzene in the absence of COD (Figure S16); (iii) these radicals react onwards in the presence of COD to generate different radical species (Figure S17); and (iv) under these conditions **5** is ultimately produced.

Moreover, the key role of magnesium complex **2** in giving rise to the radical species from which **5** is produced is emphasized by the fact that independently prepared samples of (NON)Al–Al(NON) neither generate detectable radical species (as shown by EPR spectroscopy) nor react with COD under comparable photolysis conditions in benzene. Attempts to capture the radical species photolytically

generated from **2** via the use of other radical traps are currently ongoing.

In conclusion, we report on the synthesis of a homoleptic magnesium bis(alumanyl) compound, which acts a four electron reservoir in the reductive defluorination of SF<sub>6</sub>, and which reacts thermally with polar substrates such as methyl iodide via nucleophilic attack through aluminium, consistent with the QT-AIM charges calculated for the metal centres and a *formal* description as a Al(I)–Mg(II)–Al(I) trimetallic. By contrast, under photolytic activation, the reaction with 1,5-cyclooctadiene leads to the stereoselective generation of transannular cycloaddition products consistent with radical based chemistry, emphasizing the covalent nature of the Mg–Al bonds and a description as a Al(II)–Mg(0)–Al(II) synthon.<sup>[26]</sup>

### Acknowledgements

We thank the EPSRC Centre for Doctoral Training in Inorganic Chemistry for Future Manufacturing (OxICFM; EP/S023828/1) and the Leverhulme Trust (RP-2018-246) for funding. ME thanks the Alexander von Humboldt Stiftung for a Feodor Lynen Fellowship. The authors would like to acknowledge the use of the University of Oxford Advanced Research Computing (ARC) facility in carrying out this work.

### Conflict of Interest

The authors declare no conflict of interest.

### Data Availability Statement

The data that support the findings of this study are available in the supplementary material of this article.

**Keywords:** aluminium · magnesium · main group chemistry · nucleophile · radical

- [1] *Molecular Metal-Metal Bonds: Compounds, Synthesis, Properties*, ed. S. T. Liddle, Wiley-VCH, Weinheim **2015**, chps 2, 12–15.
- [2] Selected reviews: a) P. P. Power, *Organometallics* **2007**, *26*, 4362–4372; b) F. Hanusch, L. Groll, S. Inoue, *Chem. Sci.* **2021**, *12*, 2001–2015.
- [3] a) P. P. Power, *Nature* **2010**, *463*, 171–177; b) C. Weetman, S. Inoue, *ChemCatChem* **2018**, *10*, 4213–4228.
- [4] a) M. Stender, A. D. Phillips, R. J. Wright, P. P. Power, *Angew. Chem. Int. Ed.* **2002**, *41*, 1785–1787; b) A. D. Phillips, R. J. Wright, M. M. Olmstead, P. P. Power, *J. Am. Chem. Soc.* **2002**, *124*, 5930–5931; c) G. H. Spikes, J. C. Fettinger, P. P. Power, *J. Am. Chem. Soc.* **2005**, *127*, 12232–12233; d) Y. Peng, M. Brynda, B. D. Ellis, J. C. Fettinger, E. Rivard, P. P. Power, *Chem. Commun.* **2008**, 6042–6044.
- [5] I. Resa, E. Carmona, E. Gutierrez-Puebla, A. Monge, *Science* **2004**, *305*, 1136–1138.

- [6] a) S. P. Green, C. Jones, A. Stasch, *Science* **2007**, *318*, 1754–1757; b) C. Jones, *Nat. Chem. Rev.* **2017**, *1*, 0059.
- [7] Zn<sub>3</sub> and MZn<sub>2</sub> (M=Cd, Hg) systems: a) M. P. Blake, N. Kaltsoyannis, P. Mountford, *Chem. Commun.* **2015**, *51*, 5743–5746; b) J. Hicks, E. J. Underhill, C. E. Kefalidis, L. Maron, C. Jones, *Angew. Chem. Int. Ed.* **2015**, *54*, 10000–10004; c) C. Bakewell, B. J. Ward, A. J. P. White, M. R. Crimmin, *Chem. Sci.* **2018**, *9*, 2348–2356.
- [8] Mg<sub>3</sub> system: B. Rösch, T. X. Gentner, J. Eyselien, J. Langer, H. Elsen, S. Harder, *Nature* **2021**, *592*, 717–721.
- [9] MGa<sub>2</sub> systems: a) A. Kempter, C. Gemel, T. Cadenbach, R. A. Fischer, *Inorg. Chem.* **2007**, *46*, 9481–9487; b) G. Prabusankar, C. Gemel, M. Winter, R. W. Seidel, R. A. Fischer, *Chem. Eur. J.* **2010**, *16*, 6041–6047.
- [10] ZnAl<sub>2</sub> system: J. Weßing, C. Göbel, B. Weber, C. Gemel, R. A. Fischer, *Inorg. Chem.* **2017**, *56*, 3517–3525.
- [11] For a recent *f*-block example, see: G. Feng, F. L. Chan, Z. Lin, M. Yamashita, *J. Am. Chem. Soc.* **2024**, ASAP. DOI: 10.1021/jacs.4c01193.
- [12] See, for example C. Jones, D. P. Mills, J. A. Platts, R. P. Rose, *Inorg. Chem.* **2006**, *45*, 3146–3148.
- [13] a) J. Hicks, P. Vasko, J. M. Goicoechea, S. Aldridge, *Nature* **2018**, *557*, 92–95; b) J. J. Schwamm, M. D. Anker, M. Lein, M. P. Coles, *Angew. Chem. Int. Ed.* **2019**, *58*, 1489–1493; c) J. Hicks, P. Vasko, J. M. Goicoechea, S. Aldridge, *J. Am. Chem. Soc.* **2019**, *141*, 11000–11003; d) S. Kurumada, S. Takamori, M. Yamashita, *Nat. Chem.* **2020**, *12*, 36–39; e) K. Koshino, R. Kinjo, *J. Am. Chem. Soc.* **2020**, *142*, 9057–9062; f) R. J. Schwamm, M. P. Coles, M. S. Hill, M. F. Mahon, C. L. McMullin, N. A. Rajabi, A. S. S. Wilson, *Angew. Chem. Int. Ed.* **2020**, *59*, 3928–3932; g) S. Grams, J. Eyselien, J. Langer, C. Färber, S. Harder, *Angew. Chem. Int. Ed.* **2020**, *59*, 15982–15986; h) S. Grams, J. Mai, J. Langer, S. Harder, *Organometallics* **2022**, *41*, 2862–2867; i) G. Feng, K. L. Chan, Z. Lin, M. Yamashita, *J. Am. Chem. Soc.* **2022**, *144*, 22662–22668; j) C. Yan, R. Kinjo, *Angew. Chem. Int. Ed.* **2022**, *61*, e202211800; k) R. A. Jackson, A. J. R. Matthews, P. Vasko, M. F. Mahon, J. Hicks, D. Liptrot, *Chem. Commun.* **2023**, *59*, 5277–5280; l) D. Sarkar, P. Vasko, A. F. Roper, M. M. D. Roy, A. E. Crumpton, L. P. Griffin, C. Bogle, S. Aldridge, *manuscript submitted*.
- [14] a) J. Hicks, A. Mansikkamäki, P. Vasko, J. M. Goicoechea, S. Aldridge, *Nat. Chem.* **2019**, *11*, 237–241; b) K. Sugita, M. Yamashita, *Chem. Eur. J.* **2020**, *26*, 4520–4523; c) H. Y. Liu, R. J. Schwamm, M. S. Hill, M. F. Mahon, C. F. McMullin, N. A. Rajabi, *Angew. Chem. Int. Ed.* **2021**, *60*, 14390–14393; d) C. McManus, J. Hicks, X. Cui, L. Zhao, G. Frenking, J. M. Goicoechea, S. Aldridge, *Chem. Sci.* **2021**, *12*, 13458–13468; e) M. M. D. Roy, J. Hicks, P. Vasko, A. Heilmann, A.-M. Baston, J. M. Goicoechea, S. Aldridge, *Angew. Chem. Int. Ed.* **2021**, *60*, 22301–22306; f) M. J. Evans, G. H. Iliffe, S. E. Neale, C. L. McMullin, J. R. Fulton, M. D. Anker, M. P. Coles, *Chem. Commun.* **2022**, *58*, 10091–10094.
- [15] *Molecules and Models: The Molecular Structures of Main Group Element Compounds*, A. Haaland, OUP, Oxford **2008**, chp 10.
- [16] T. Schwabe, S. Grimme, *Phys. Chem. Chem. Phys.* **2007**, *9*, 3397–3406.
- [17] B. Cordero, V. Gómez, A. E. Platero-Prats, M. Revés, J. Echeverría, E. Cremades, F. Barragán, S. Alvarez, *Dalton Trans.* **2008**, 2832–2838.
- [18] For previous examples of Mg–Al covalent bonds see refs 7c, 13a, 13f, 14e and 14f, plus: a) A. Paparo, C. D. Smith, C. Jones, *Angew. Chem. Int. Ed.* **2019**, *58*, 11459–11463; b) S. Brand, H. Elsen, J. Langer, S. Grams, S. Harder, *Angew. Chem. Int. Ed.* **2019**, *58*, 15496–15503; c) A. Friedrich, J. Eyselien, J. Langer, C. Färber, S. Harder, *Angew. Chem. Int. Ed.* **2021**, *60*, 16492–16499.

- [19] *Atoms in Molecules: A Quantum Theory*, R. Bader, OUP, Oxford **1994**.
- [20] See also: D. J. Sheldon, M. R. Crimmin, *Chem. Commun.* **2021**, 7, 7096–7099.
- [21] *Chemistry of the Elements*, N. N. Greenwood, A. Earnshaw, 2nd edition, Elsevier, Amsterdam **1997**.
- [22] Hydrolysis of **5** with weak acids generates the parent hydrocarbon *cis*bicyclo[3.3.0]octane: W. B. Moniz, J. A. Dixon, *J. Am. Chem. Soc.* **1961**, 83(7), 1671–1675.
- [23] Early reports of the stereoselective transannular radical cyclization of 1,5-cyclooctadiene to *cis*bicyclo[3.3.0]octanes: a) R. Dowbenko, *J. Am. Chem. Soc.* **1964**, 86, 946–947; b) L. Friedman, *J. Am. Chem. Soc.* **1964**, 86, 1885–1886; c) R. Dowbenko, *Tetrahedron* **1964**, 20, 1843; d) J. D. Winkler, V. Sridar, *J. Am. Chem. Soc.* **1986**, 108, 1708–1709.
- [24] E. C. Ashby, T. N. Pham, *J. Org. Chem.* **1986**, 51, 3598–3602.
- [25] For a previous report of potential Al(II) radical species see: D. Mandal, T. I. Demirer, T. Sergeieva, B. Morgenstern, H. T. A. Wiedemann, C. W. M. Kay, D. M. Andrada, *Angew. Chem. Int. Ed.* **2023**, 62, e202217184.
- [26] Details of the X-ray crystal structures described in this paper are available from the CCDC, deposition numbers 2219353, 2219355–2219358 and 2221942.

Manuscript received: March 13, 2024

Accepted manuscript online: March 27, 2024

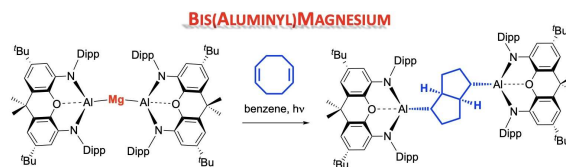
Version of record online: ■■, ■■

## Zuschriften

## Main Group Chemistry

L. P. Griffin, M. A. Ellwanger, J. Clark,  
W. K. Myers, A. F. Roper, A. Heilmann,  
S. Aldridge\* [e202405053](#)

Bis(Aluminyl)Magnesium: a Source of Nucleophilic or Radical Aluminium-Centred Reactivity



NON-LINEAR STRUCTURE  
 FOUR-ELECTRON REDUCTANT

NUCLEOPHILIC ALUMINIUM  
 PHOTOLYTIC RADICAL CHEMISTRY

The magnesium bis(aluminyl) compound  $\text{Mg}[\text{Al}(\text{NON})]_2$  reacts thermally with MeI via nucleophilic attack through Al, consistent with a *formal* description as an Al(I)–Mg(II)–Al(I) trimetallic species. Under photolytic activation, reac-

tion with 1,5-cyclooctadiene leads to the transannular cycloaddition products, consistent with radical chemistry, emphasizing the covalent nature of the Mg–Al bonds and a description as an Al(II)–Mg(0)–Al(II) synthon.